NIH Public Access
Author Manuscript
Bioorg Med Chem. Author manuscript; available in PMC 2011 May 5.

Published in final edited form as:
Bioorg Med Chem. 2009 September 15; 17(18): 6496–6504. doi:10.1016/j.bmc.2009.08.016.

Synthesis, Structure-Affinity Relationships and Modeling of AMDA Analogs at 5-HT_{2A} and H_1 Receptors: Structural Factors Contributing to Selectivity

Jitesh R. Shah[a], **Philip D. Mosier**[a], **Bryan L. Roth**[b], **Glen E. Kellogg**[a], and **Richard B. Westkaemper**[a,*]

[a] Department of Medicinal Chemistry, School of Pharmacy, Virginia Commonwealth University, Richmond, VA 23298 USA

[b] Department of Pharmacology, University of North Carolina School of Medicine, Chapel Hill, NC 27599 USA

Abstract

Histamine H_1 and serotonin 5-HT_{2A} receptors present in the CNS have been implicated in various neuropsychiatric disorders. 9-Aminomethyl-9,10-dihydroanthracene (AMDA), a conformationally constrained diarylalkyl amine derivative, has affinity for both of these receptors. A structure-affinity relationship (SAFIR) study was carried out studying the effects of *N*-methylation, varying the linker chain length and constraint of the aromatic rings on the binding affinities of the compounds with the 5-HT_{2A} and H_1 receptors. Homology modeling of the 5-HT_{2A} and H_1 receptors suggests that AMDA and its analogs, the parent of which is a 5-HT_{2A} antagonist, can bind in a fashion analogous to that of classical H_1 antagonists whose ring systems are oriented towards the fifth and sixth transmembrane helices. The modeled orientation of the ligands are consistent with the reported site-directed mutagenesis data for 5-HT_{2A} and H_1 receptors and provide a potential explanation for the selectivity of ligands acting at both receptors.

Keywords

5-HT_{2A} receptor; H_1 receptor; Phenylethylamines; 9-Aminoalkyl-9,10-dihydroanthracene (AMDA); G Protein-Coupled Receptor (GPCR); Structure-Activity Relationship (SAR); Structure-Affinity Relationship (SAFIR)

1. Introduction

Sleep disorders and circadian rhythm abnormalities are prevalent, with 70 million Americans reporting disturbed sleep each year. Epidemiological studies indicate that between 30–48% of the global population find difficulty in initiating and maintaining sleep.[1] Serotonin (5-hydroxytryptamine, 5-HT), a major neurotransmitter found in the CNS and periphery, has been reported to be involved in the control of sleep and waking states.[2] 5-HT_2

© 2009 Published by Elsevier Ltd.

Correspondence: Richard B. Westkaemper, Department of Medicinal Chemistry, P. O. Box 980540, School of Pharmacy, Virginia Commonwealth University, Richmond, VA 23298-0540, rbwestka@vcu.edu, Telephone: (804)828-6449, FAX: (804)828-7625.

Publisher's Disclaimer: This is a PDF file of an unedited manuscript that has been accepted for publication. As a service to our customers we are providing this early version of the manuscript. The manuscript will undergo copyediting, typesetting, and review of the resulting proof before it is published in its final citable form. Please note that during the production process errors may be discovered which could affect the content, and all legal disclaimers that apply to the journal pertain.

NIH-PA Author Manuscript
NIH-PA Author Manuscript
NIH-PA Author Manuscript

NIH-PA Author Manuscript

NIH-PA Author Manuscript

NIH-PA Author Manuscript

receptors belong to the superfamily of G protein-coupled receptors (GPCRs) and consist of three subtypes: 2A, 2B and 2C. 5-HT_{2A} receptors are involved mainly in non-rapid eye movement sleep regulation and respiratory control,[3] and selective antagonism of the 5-HT_{2A} receptor has emerged as a promising new mechanism for the treatment of sleep disorders.[4]

Histamine released by tissue mast cells, basophils and histaminergic neurons is also known to impact the ability to fall asleep and stay asleep.[5] It has been suggested that ligands acting at H_1 receptors in the CNS may be useful in the treatment of neuropsychiatric and sleep disorders.[6] Histamine exerts its effect by interacting with four different receptors H_1-H_4, which are GPCRs.[7,8] Early research and development of H_1 ligands has focused largely on antagonists that are used for their antiallergic effects in the periphery. However, first-generation H_1 receptor antagonists (diphenhydramine, mepyramine, chlorpheniramine) also exhibit high H_1 receptor occupancy in the CNS due in part to their lipophilicity, leading to sedative effects.[9–11] This led to the development of second-generation antagonists (acrivastine, loratadine, terfenadine, cetirizine, etc.) that exhibited high selectivity and less sedative potential due to the decrease in their ability to penetrate the blood brain barrier.[12,13] Some of these antagonists (doxepin, ketotifen, epinastine, olopatadine), which have a tri- or tetracyclic fused ring system, also showed affinity at 5-$HT_{2A,}$ adrenaline α_1, dopamine D_2 and muscarinic M_1 receptors, indicative of their low selectivity for the H_1 receptor.[14] Among the various chemical classes of H_1 antagonists, ligands that are zwitterionic (olopatadine, acrivastine, fexofenadine) showed the highest degree of selectivity for H_1, suggesting that the carboxylate group of the ligand may interact with a residue (K191)[15] in the H_1 receptor that is not present in the other GPCRs. Introduction of a carboxylate moiety thus provides one potential means of designing peripherally-acting H_1-selective antagonists.

In this study, we set out to determine if H_1 versus 5-HT_{2A} selectivity could be achieved through the systematic modification of the uncharacteristically nonpolar[16] structure of 9-(aminomethyl)-9,10-dihydroanthracene (AMDA, **1a**). We have previously reported AMDA as the parent member of a potentially new class of high-affinity 5-HT_{2A} antagonists.[17,18] This work builds on our earlier studies[19] by creating a “matrix” of AMDA-like compounds in which the aromatic ring system, degree of *N*-methylation and length of the aliphatic linker are systematically varied. A series of 9-(aminoalkyl)-9,10-dihydroanthracenes (DHAs) and an analogous series of diphenylalkylamines (DPAs) were synthesized and their binding affinities at H_1 and 5-HT_{2A} determined. Our results show that AMDA and related compounds exhibit varying degrees of affinity for the H_1 receptor. Homology models using the human β_2-adrenoceptor (β_2-AR)[20] as a template provide receptor-based explanations for the observed structure-affinity relationships (SAFIR) among the AMDA analogs. To our knowledge this is also the first report of a comparison of 5-HT_{2A} and H_1 homology models generated from the β_2-adrenergic structure.

2. Results and discussion

2.1. Chemistry

9-(Aminomethyl)-9,10-dihydroanthracene (**1a**), 9-(2-aminoethyl)-9,10-dihydroanthracene (**2a**) and 9-(2-aminopropyl)-9,10-dihydroanthracene (**3a**) were prepared as previously described.[19,21] *N*-Alkylated analogs **1b, 1c, 3b** and **3c** have been reported by us.[19] *N*-Methylated analogs of **2a** were synthesized (Scheme 1) using 9-hydroxymethylanthracene **7** as the starting material. Halogenation[22] followed by cyanation[23] of the alcohol gave 2-(anthracen-9-yl)acetonitrile **9** that was further hydrolyzed to the corresponding acid **10**. Anthracene ring reduction using sodium metal in *n*-pentanol gave 2-(9,10-dihydroanthracen-9-yl)acetic acid (**11**). Sequential conversion of the acid **11** to its amide **12** via acid chloride, followed by reduction, afforded 2-(9,10-dihydroanthracen-9-yl)-*N*-methylethanamine (**2b**). 2-(9,10-Dihydroanthracen-9-yl)-*N*,*N*-dimethylethanamine (**2c**) was

NIH-PA Author Manuscript

NIH-PA Author Manuscript

NIH-PA Author Manuscript

obtained by reductive amination[24] of 2-(9,10-dihydroanthracen-9-yl)acetaldehyde (**15**), which was obtained by the oxidation of 2-(9,10-dihydroanthracen-9-yl)ethanol (**14**) (Scheme 2). *N*-Methyl-2,2-diphenylethanamine[25] (**4b**) was obtained by the *N*-methylation of the respective amine as reported.[26] *N*,*N*-Dimethyl-3,3-diphenylpropan-1-amine[27] (**5c**) was obtained by the same method adopted for the synthesis of **2c** from commercially available 3,3-diphenylpropanal. 4,4-Diphenylbutan-1-amine[28] (**6a**) was obtained by the BH_3·THF reduction of commercially available 4,4-diphenylbutanenitrile. Compounds **4a**, **4c**, **5a**, **5b**, **6b**, and **6c** were commercially obtained.

2.2. Structure-affinity relationships

Several reviews describing structure-activity relationship studies of diphenhydramine-like antihistamines have been reported.[29–31] The features that have been systematically varied include the nature of the two required aromatic groups, the terminal basic amine and the aliphatic linker between these two features.[32,33] In this work, we examined similar structural variations using AMDA as the parent structure. These compounds closely resemble well-established H_1 antagonists: replacement of the ether oxygen of diphenhydramine by a methylene unit results in compound **6c** and replacement of the pyridin-2-yl group of the H_1 antagonist pheniramine with a phenyl group results in **5c**.

Compound affinities for the 5-HT_{2A} and H_1 receptors are given in Table 1 and displayed graphically in Fig. 1. The most significant differences in affinity were observed between the 9-(aminoalkyl)-9,10-dihydroanthracene (DHA) compounds (Fig. 1a) and their corresponding diphenylalkylamine (DPA) congeners (Fig. 1b). Ring-opening of the tricyclic system uniformly produced decreases in affinity for both 5-HT_{2A} and H_1 receptors. No DPA compound exhibited high affinity (K_i < 100 nM) at 5-HT_{2A}, and only three showed high affinity for H_1 receptors (**5b**, K_i = 64 nM; **5c**, K_i = 75 nM; **6c**, K_i = 70 nM). In contrast, many of the DHA analogs were found to have high affinity at both receptors, demonstrating that dihydroanthracene is a privileged[34] structure. For compounds interacting with the H_1 receptor, progressively increasing either the number of methylene units in the linker or the number of *N*-methyl groups consistently retained or enhanced affinity in both the DHA and the DPA series. H_1 receptor affinity was insensitive to chain length for the unsubstituted amine analogs of AMDA (**1a**, K_i = 197 nM; **2a**, K_i = 137 nM; **3a**, K_i = 175 nM). In contrast, H_1 affinity increased with increasing chain length for both *N*-methylated (**1b**, K_i = 189 nM; **2b**, K_i = 48 nM; **3b**, K_i = 3 nM) and *N*,*N*-dimethylated analogs (**1c**, K_i = 25 nM; **2c**, K_i = 6 nM; **3c**, K_i = 0.5 nM). For the DHA analogs, *N*,*N*-dimethylation and a three-methylene linker was optimal for H_1 affinity (**3c**, K_i = 0.5 nM). The trends in affinity at 5-HT_{2A} are less uniform. Like the H_1 receptor, the affinity of the DPA compounds for 5-HT_{2A} generally increased with increasing linker length or degree of *N*-methylation though, as noted above, no DPA compound was found to have substantial (K_i < 700 nM) affinity for the 5-HT_{2A} receptor. As observed previously for DHA[19] and compounds with a one-methylene linker, 5-HT_{2A} affinity decreased as *N*-methylation degree increased (**1a**, K_i = 20 nM; **1b**, K_i = 52 nM; **1c**, K_i = 540 nM). This trend was not observed for the other linker lengths. Additionally, for DHA compounds with no *N*-methylation, linker lengths of one (**1a**, K_i = 20 nM) and three (**3a**, K_i = 32 nM) methylene units demonstrated significantly higher affinity than the two-methylene linker (**2a**, K_i = 480 nM) compound. Affinities were more uniform for compounds with one *N*-methyl group (**1b**, K_i = 52 nM; **2b**, K_i = 92 nM; **3b**, K_i = 13 nM), and for those with two *N*-methyl groups, affinity increased with linker length by 25-fold (**1c**, K_i = 540 nM; **2c**, K_i = 84 nM; **3c**, K_i = 22 nM). In general, 5-HT_{2A} receptor affinity is less sensitive to *N*-methylation and chain length variation than H_1 receptor affinity.

NIH-PA Author Manuscript

NIH-PA Author Manuscript

NIH-PA Author Manuscript

2.3. Modeling receptor-ligand interactions

2.3.1. H_1 and 5-HT_{2A} receptor models—When considering the selectivity of a particular ligand for one receptor versus another, it is useful to analyze the differences in amino acids that comprise the binding sites of the two receptors. The alignment of the human H_1 and 5-HT_{2A} receptor sequences with that of human β_2-AR is presented in Fig. 2. The H_1 receptor is phylogenetically related to the 5-HT_2 receptor subtypes, with higher sequence homology found primarily in the transmembrane-spanning regions.[35] Based on the primary sequences, binding site analysis of both 5-HT_{2A} and H_1 receptors indicates that the major variations in amino acid constitution occur at positions 3.33, xl2.52, xl2.54, 5.39, 5.42, 6.55 and 7.35 (Fig. 2). Differences in steric and electrostatic sidechain properties at these and other positions are likely responsible for directing the ligand selectivity of the two receptors. The H_1 receptor amino acid residue K191$^{5.39}$, not commonly found at this position among aminergic GPCRs, could be potentially exploited for the design of highly selective H_1 ligands. The three-dimensional arrangement of these residues is shown in Fig. 3. The residues that are conserved between H_1 and 5-HT_{2A} are those that tend to be highly conserved among all aminergic GPCRs. These residues, primarily located in the inner region of the binding cavity, include W$^{3.28}$, the amine counter-ion D$^{3.32}$, S$^{3.36}$ and T$^{3.37}$, and the 'aromatic cluster' [36–39] residues W$^{6.48}$ and F$^{6.52}$, and Y$^{7.43}$ (an H-bonding partner for D$^{3.32}$).

Models of human H_1 and 5-HT_{2A} receptors were generated with the MODELLER[40] program using a high-resolution crystal structure of the human β_2-AR[20] as the template (see Experimental Methods). Inspection of putative receptor binding sites and ligand binding modes in our homology models (Figs. 4 and 5) indicate two common interactions that occur for each of the compounds listed in Table 1 at both 5-HT_{2A} and H_1 receptors: 1) the highly conserved aspartic acid residue at position[41] 3.32 (H_1, D107$^{3.32}$; 5-HT_{2A}, D155$^{3.32}$) is able to interact with the protonated amine of the docked ligand; and 2) hydrophobic residues present in transmembrane helix 6 (TM6) comprising the aromatic cluster[42] are able to interact with the aromatic rings of the ligands. In other binding site locations variability of amino acid residues at equivalent positions in the hH_1 and h5-HT_{2A} receptors influence the way the aromatic rings are oriented in the receptor, which in turn provides an explanation for the observed differences in affinity for AMDA and its analogs with varying chain lengths. The presence of hydrophobic residues surrounding the conserved D$^{3.32}$ in H_1 and in 5-HT_{2A}, together with the aromatic cluster region in H_1 and in 5-HT_{2A}, provide sites of favorable interaction with the ligands for each receptor.

2.3.3. Binding mode analysis—Compounds listed in Table 1 were docked into the receptor binding sites of the H_1 and 5-HT_{2A} receptor models using the GOLD automated docking routine.[43] The GOLD scoring function (steric and electrostatic interactions) was used to select the favored ligand conformation. In addition, we carried out HINT[44] (Hydropathic INTeraction) analysis to characterize the nature of the binding site interactions. HINT is a free-energy-based method that considers atom-atom interactions in a bimolecular complex using a parameter set derived from octanol/water partition coefficients.[45] Modeling observations indicate that the compounds prefer to be oriented within the binding pockets of the two receptor models in similar, but distinct binding modes (see Figures 4 and 5). The well-known aspartate D$^{3.32}$ residue was found to interact with the basic amine in both receptors for each docked ligand, and the ligand aromatic rings were consistently oriented in the binding site surrounded by TM4, TM5 and TM6. In general, for the short-chain linker ligands there is a relatively small amount of ligand surface area that may interact with the surrounding hydrophobic environment in the binding pocket, accounting for the observed decreased affinity of these compounds at both 5-HT_{2A} and H_1

NIH-PA Author Manuscript

NIH-PA Author Manuscript

NIH-PA Author Manuscript

(Figs. 4c and 5c). However, for AMDA (**1a**), the observed high affinity could be due to the presence of an alternate binding mode.[46]

The tricyclic DHA ring system in **3c** showed strong hydrophobic interactions (Y108$^{3.33}$, L163$^{4.61}$, F168$^{xl2.38}$, F190$^{5.38}$ and F435$^{6.55}$), with the phenyl rings oriented toward TM5 and the aliphatic linker located deep in the H_1 binding pocket. In contrast, in the 5-HT_{2A} model, **3c** is oriented such that the phenyl rings are facing TM6 (F339$^{6.51}$, F340$^{6.52}$ and N343$^{6.55}$) and the aliphatic linker is positioned closer to extracellular loop 2 (EL2). For both H_1 and 5-HT_{2A}, the compound with the longest linker and highest degree of methylation (**3c**) was found to have the highest (H_1) or one of the highest (5-HT_{2A}) affinities among the compounds tested. The methylene linkers in the H_1 receptor are able to interact with residues L104$^{3.29}$ and Y431$^{6.51}$, which explains the comparatively higher affinity of **3c** for H_1 than for 5-HT_{2A}. Further, the observed differences in ligand orientation within the receptor binding site can account for the preference for *N*-methylation at H_1, with the methyl groups more closely surrounded by hydrophobic residues as compared to 5-HT_{2A} (Figs. 4a and 5a).

For the unbridged DPA analogs, the increased conformational flexibility (as compared to DHA) and intramolecular steric repulsion produce a twisted ring orientation. This results in more unfavorable receptor-ligand interactions (steric clashes and polar-nonpolar interactions) involving the ring system and the surrounding residues (Figs. 4b and 5b).

HINT hydropathic interaction analysis provided additional support for the proposed orientation of the ligands in the binding pocket. Fig. 6 shows the HINT maps generated for compound **3c** (which has the highest affinity for both receptors) in the binding sites of the H_1 and 5-HT_{2A} receptors. In each case the tricyclic ring system fits into the hydrophobic 'aromatic cluster' while the amine group faces D107$^{3.32}$ and is stabilized by both ionic and hydrogen bonding interactions. However, both the aliphatic linker region and the *N*-methyl groups engage in more extensive hydrophobic interactions in H_1 than in 5-HT_{2A}.

In addition, the receptor-ligand complexes described here are in general agreement with other studies that have implicated residues that contribute to an antagonist binding site in H_1 and 5-HT_{2A}. Besides the several key residues that have been reported by site-directed mutagenesis studies in H_1 receptor models[15,47] (W158$^{4.56}$, Y200$^{5.48}$, F424$^{6.44}$, W428$^{6.48}$, F432$^{6.52}$ and F435$^{6.55}$) and 5-HT_{2A} receptor models[48] (F243$^{5.47}$, W336$^{6.48}$, F339$^{6.51}$, F340$^{6.52}$), we found that Y108$^{3.33}$ and I454$^{7.39}$ were oriented to favorably interact with ligands in the binding pocket of the H_1 receptor, and the cognate residues V156$^{3.33}$ and V366$^{7.39}$ for the 5-HT_{2A} receptor. The differences in the stereoelectronic character of these residues likely contribute to the differences in the way the ligand binds to these receptors, and consequently the observed differences in binding affinity.

3. Conclusions

Within the matrix of compounds synthesized and tested, the *N*,*N*-dimethylated chain-lengthened propylene analog of AMDA shows the highest affinity at both 5-HT_{2A} and H_1 receptors (**3c**: 5-HT_{2A}, K_i = 22 nM; H_1, K_i = 0.5 nM) and the highest selectivity for the H_1 receptor (44-fold). In addition, removing the conformational restriction of the dihydroanthracene tricyclic system by ring-opening to provide a diphenyl system is detrimental to the ligand affinity for both 5-HT_{2A} and H_1 receptors. Structure-affinity relationships among these compounds show that *N*-alkylation either decreases or has little effect on 5-HT_{2A} affinity, while the propylene linker is the optimum chain length between the tricyclic system and amine for receptor affinity. Modeling studies suggest that diaryl alkylamine analogs exhibit a common binding mode within the 5-HT_{2A} and H_1 receptors.

NIH-PA Author Manuscript

NIH-PA Author Manuscript

NIH-PA Author Manuscript

Hydropathic analysis of the modeled complexes supports the proposed role of the TM6 aromatic cluster in directing binding. The proposed differences in the binding pocket of H_1 ($Y108^{3.33}$ and $I454^{7.39}$) and 5-HT_{2A} ($V156^{3.33}$ and $V366^{7.39}$) may determine the way ligands bind, which in turn may determine the selectivity of the ligands for each of the two receptors. These preliminary modeling results provide a qualitative understanding of how AMDA analogs might interact with the 5-HT_{2A} and H_1 receptors. This study also provides potential insight into the mechanisms by which differences in the structures of the receptors and ligands determines receptor selectivity. We continue to synthesize and test compounds and refine our models toward the development of a more quantitative and predictive structure-based QSAR model.

4. Experimental

4.1. Chemistry

Nuclear magnetic resonance (^{1}H NMR and ^{13}C NMR) spectra were recorded using a Varian Gemini 300 spectrometer in $CDCl_3$ using tetramethylsilane as an internal standard unless otherwise specified. Melting points were determined using an OptiMelt melting point apparatus and are uncorrected. Elemental analyses were performed by Atlantic Microlab, Inc., and determined values are within 0.4% of theory. All reactions were maintained under a nitrogen atmosphere. Anhydrous solvents were purchased and stored under nitrogen over molecular sieves. Medium-pressure column chromatography was carried out using silica gel 60 Å, 0.040–0.063 mm, (200–400 mesh), Sorbent Technologies.

4.1.1. 9-Bromomethylanthracene (8).[22]—Phosphorus tribromide (0.8 ml, 8.4 mmol) was added to a suspension of 9-hydroxymethylanthracene **7** (1.5 g, 7.2 mmol) in toluene (40 ml) at 0 °C *via* syringe. The mixture was stirred at 0 °C for 1 h and then warmed to rt, during which the reaction became homogeneous. Saturated Na_2CO_3 solution (15 mL) was added slowly and the reaction mixture was stirred until it cooled to rt. The phases were separated, and the organic phase was washed with H_2O (10 mL), brine (10 mL) and dried over $MgSO_4$. The yellow filtrate was concentrated to minimum volume, and then stored at 0 °C for crystallization. The yellow needle-like solid was collected and dried in vacuum (1.24 g). The mother liquid was concentrated and purified using medium pressure column chromatography (0.6 g). The two parts were combined to give the product **8** (total 1.84 g, 94%) as yellow solid. mp 143 – 146 °C. ^{1}H NMR (300 MHz, $CDCl_3$): δ 5.3 (s, 2H, CH_2-Br), 7.2 – 8.3 (m, 9H, Ar-H). ^{13}C NMR (75 MHz, $CDCl_3$): δ 32.20, 125.50, 125.70, 125.80, 127.70, 128.10, 129.40, 131.60.

4.1.2. 2-(Anthracen-9-yl)acetonitrile (9)—A solution of 9-bromomethylanthracene **8** (1.5 g, 5.53 mmol) in DMSO (15 mL) was added over 10 min to a stirred suspension of KCN (0.54 g, 8.29 mmol) in DMSO (30 mL) at 70 °C under N_2. The mixture was stirred for an additional 40 min, cooled to rt, and diluted with H_2O. The aqueous layer was saturated with NaCl and then extracted with ether (3 × 25 mL). The combined extracts were washed with H_2O, dried ($MgSO_4$), filtered, and concentrated to yield solid product **9** (0.96 g, 80%). mp 154 – 156 °C. ^{1}H NMR (300 MHz, $CDCl_3$): δ 4.6 (s, 2H, CH_2-CN), 7.2–8.5 (m, 9H, Ar-H). ^{13}C NMR (75 MHz, $CDCl_3$): δ 20.50, 125.20, 125.31, 124.60, 126.10, 128.20, 130.10, 131.60.

4.1.3. 2-(Anthracen-9-yl)acetic acid (10)—KOH (0.97 g, 17.48 mmol) in 10 ml of H_2O was added to a suspension of 2-(anthracen-9-yl)acetonitrile **9** (0.95 g, 4.37 mmol) in ethylene glycol (50 ml). The mixture was heated at reflux for 24 h until homogenous. The hot solution was filtered, and the filtrate was acidified with dilute HCl to obtain the precipitated product **10** (1.0 g, 100%). mp 228 – 230 °C. ^{1}H NMR (300 MHz, $CDCl_3$): δ 4.2

NIH-PA Author Manuscript

NIH-PA Author Manuscript

NIH-PA Author Manuscript

(s, 2H, CH_2), 7.5 – 8.5 (m, 9H, Ar-H). ^{13}C-NMR (75 MHz, $CDCl_3$): δ 34.20, 124.60, 125.30, 125.60, 126.10, 128.20, 130.50, 131.90, 173.40.

4.1.4 2-(9,10-Dihydroanthracen-9-yl)acetic acid (11)—Sodium metal (10 equiv) was added slowly to a refluxing solution of 2-(anthracen-9-yl)acetic acid **10** (0.9 g, 3.8 mmol) in 1-pentanol (20 ml). The reaction mixture was stirred for 10 min until all of the sodium dissolved, then was cooled and H_2O (10 mL) was added. The solution was made acidic with 5% HCl. The reaction mixture was concentrated under vacuum and the oily solution obtained was triturated with chloroform, dried ($MgSO_4$) and concentrated to yield pure product **4** (0.76 g, 84%). ^{1}H NMR (300 MHz, $CDCl_3$): δ 2.8 (d, *J* = 7.8 Hz 2H, CH_2), 4.4 (t, *J* = 7.8 Hz, 1H, CH), 3.9 (d, *J* = 18.1 Hz, 2H, Ar-CH_2-Ar), 4.1 (d, *J* = 18.1 Hz, 2H, ArCH_2-Ar), 7.1–7.3 (m, 8H, Ar-H). ^{13}C-NMR (75 MHz, $CDCl_3$): δ 40.1, 41.2, 45.1, 126.8, 128.7, 138.4, 139.6, 177.4.

4.1.5. 2-(9,10-Dihydroanthracen-9-yl)-*N*-methylacetamide (12)—Thionyl chloride (1.73 g, 14.6 mmol) was added under N_2 to a stirred solution of compound **11** (0.7 g, 2.9 mmol) in anhydrous benzene (5 mL). The solution was heated at reflux (2 h), allowed to cool and the excess benzene and thionyl chloride were removed under reduced pressure to provide an oil. The oil obtained was dissolved in anhydrous THF (10 mL) and cooled in an ice bath (0 °C). A methylamine/THF (2 M, 5.8 mmol) solution was added dropwise into the stirred solution, and the mixture was stirred at rt (2 h). The solvent was removed under reduced pressure to give a white solid. Water (20 mL) was added, and the suspension was extracted with EtOAc (3 × 25 mL). The combined extracts were washed with water, brine and dried ($MgSO_4$). Removal of solvent under reduced pressure gave the crude amide as a viscous oil. The resulting amide was purified using medium pressure chromatography (CH_2Cl_2/acetone, 9:1), yield (75–80%). ^{1}H NMR (300 MHz, $CDCl_3$): δ 2.45 (s, 3H, CH_3), δ 2.67 (d, *J* = 7.8 Hz, 2H, CH_2), 3.93 (d, *J* = 18.3 Hz, 2H, Ar-CH_2-Ar), 4.05 (d, *J* = 18.3 Hz, 2H, Ar-CH_2-Ar), 4.56 (t, *J* = 7.5 Hz, 1H, CH), 7.16–7.37 (m, 8H, Ar-H). ^{13}C-NMR (75 MHz, $CDCl_3$): δ 34.79, 41.0, 41.6, 42.60 126.11, 127.47, 135.91, 138.24, 176.58.

4.1.6. 2-(9,10-Dihydroanthracen-9-yl)-*N*-methylethanamine (2b)—A borane-THF complex (1.0 M in THF, 0.537 g, 6.25 mmol) was added in a dropwise manner to a stirred solution of **12 (**0.35 g, 1.25 mmol) in anhydrous THF (5 mL) under N_2 at 0 °C. The mixture was slowly warmed to rt and heated at reflux (6 h). The reaction mixture was allowed to cool to rt, and HCl (6.0 M, 3 mL) was added with caution. The mixture was heated at reflux (1 h) and allowed to cool to rt, and the solvent was removed under reduced pressure. Water was added and the residue was extracted with ether (25 mL). The aqueous portion was made basic with 10% NaOH and extracted with CH_2Cl_2 (3 × 25 mL). The organic layer was washed with water and brine, dried ($MgSO_4$), and concentrated under reduced pressure to give **2b**, which was then purified by medium pressure column chromatography. CH_2Cl_2/MeOH (9:1) yield (80–85%). mp 202 – 205 °C (oxalate). ^{1}H-NMR (300 MHz, $CDCl_3$): δ 1.81 (q, *J* = 7.5 Hz, 2H, CH_2), 2.38 (s, 3H, CH_3), 2.56 (t, *J* = 7.5 Hz, 2H, CH_2-NH), 3.89 (d, *J* = 18.3 Hz, 1H, Ar-CH_2-Ar), 4.09 (d, *J* = 18.3 Hz, 1H, Ar-CH_2-Ar), 4.03 (t, *J* = 7.2 Hz, 1H, Ar-CH-Ar), 7.1 – 7.3 (m, 8H, Ar-H). ^{13}C-NMR (75 MHz, $CDCl_3$): δ 35.30, 36.72, 37.40, 45.41, 50.20, 126.41, 128.10, 136.40, 140.61. Anal. ($C_{17}H_{19}N{\cdot}C_2H_2O_4{\cdot}0.25\ H_2O$): C, H, N.

4.1.7. 2-(9,10-Dihydroanthracen-9-yl)ethanol (14)—Na_2K silica gel (2 g) was added to a well-stirred solution of 2-(anthracen-9-yl)ethanol **13** (0.75 g, 4.4 mmol) in anhydrous THF and stirred continuously under nitrogen. The reaction mixture was refluxed for 15 min then allowed to cool to rt and quenched with H_2O (50 mL). The solid precipitate was filtered and washed with EtOAc (5 × 25 mL). The filtrate was then collected followed by extraction. The EtOAc portion was dried ($MgSO_4$) and concentrated under reduced pressure to provide

NIH-PA Author Manuscript

NIH-PA Author Manuscript

NIH-PA Author Manuscript

viscous yellow oil. The resulting yellow oil was purified using medium pressure column chromatography (CH_2Cl_2/MeOH, 9:1) to provide **14** (0.65 g, 86%) as a yellow oil. ^{1}H-NMR (300 MHz, $CDCl_3$): δ 1.86 (m, 2H, CH_2), δ 3.61 (t, 2H, CH_2-OH), 3.90 (d, *J* = 18.3 Hz, 2H, Ar-CH_2-Ar), 3.95 (d, *J* = 18.3 Hz, 1H, Ar-CH_2-Ar), 4.0 (d, *J* = 18.3 Hz, 1H, Ar-CH_2-Ar), 4.02 (t, *J* = 7.5 Hz, 1H, CH), 7.19 – 7.47 (m, 8H, Ar-H). ^{13}C-NMR (75 MHz, $CDCl_3$): δ 31.29, 31.39, 52.1, 62.30 126.11, 128.47, 137.91, 138.24.

4.1.8. 2-(9,10-Dihydroanthracen-9-yl)acetaldehyde (15)—A solution of (9,10-dihydroanthracene-9-yl)ethanol **14** (0.60 g, 1.5 mmol) dissolved in anhydrous CH_2Cl_2 (20 mL) was added to a stirred mixture of Dess-Martin oxidant (0.954 g, 2.25 mmol) in CH_2Cl_2. The reaction mixture was stirred for 1 h, then diluted with ether (75 mL) and poured into 1.3 M NaOH (75 mL). The ether layer was separated and extracted with 1.3 M NaOH (3 × 15 mL) and was washed with H_2O (2 × 20 mL), brine (20 mL), dried ($MgSO_4$) and concentrated under reduced pressure to yield an oil. The resulting oil was purified using medium pressure column chromatography (petroleum ether/EtOAc 9:1) to provide **15** (0.445 g, 75%) as an oil. ^{1}H NMR (300 MHz, $CDCl_3$): δ 2.69 (d, 2H, CH_2-CHO), 3.87 (d, *J* = 18.3 Hz, 1H, Ar-CH_2-Ar), 4.06 (d, *J* = 18.3 Hz, 1H, Ar-CH_2-Ar), 4.55 (t, *J* = 6.9 Hz, 1H, CH), 7.19 – 7.34 (m, 8H, Ar-H) 9.71 (s, 1H, CHO), ^{13}C NMR (75 MHz, $CDCl_3$): δ 34.85, 40.77, 50.0, 126.19, 127.54, 137.21, 138.50.

4.1.9. 2-(9,10-Dihydroanthracen-9-yl)-*N*,*N*-dimethylethanamine oxalate (2c)—2-(9,10-Dihydroanthracene-9-yl)acetaldehyde **15** (0.4 g, 1.79 mmol), dimethylamine hydrochloride (0.292 g, 3.59 mmol) and titanium isopropoxide (1.02 g, 3.59 mmol) were added to a solution of triethylamine (0.363 g, 3.59 mmol) in absolute ethanol. The reaction mixture was stirred at rt for 12 h. $NaBH_3$ (0.1 g, 2.68 mmol) was then added and the mixture was stirred for 12 h. The reaction was quenched by pouring the mixture into aqueous ammonia (30 mL, 2 N). The resulting precipitate was filtered and washed with CH_2Cl_2 (5 × 20 mL). The filtrate was collected and extracted with CH_2Cl_2. The CH_2Cl_2 portion was dried ($MgSO_4$) and concentrated under reduced pressure to provide viscous yellow oil. The resulting yellow oil was purified using medium pressure column chromatography (CH_2Cl_2/MeOH, 9:1) to provide **2c** (0.248 g, 55%). The yellow oil was dissolved in anhydrous acetone (10 mL) and oxalic acid (0.043 g, 0.47 mmol) was added until no further precipitate formed. The oxalate salt was recrystallized from methanol/ether to provide **2c** oxalate as pale yellow crystals. Yield (55%). mp 183 – 185 °C (oxalate). ^{1}H-NMR (300 MHz, $CDCl_3$): δ 1.83 (q, *J* = 7.5 Hz, 2H, CH_2), 2.26 (s, 6H, $(CH_3)_2$), 2.28 – 2.30 (m, 2H, CH_2-N), 3.94 (d, *J* = 18.6 Hz, 1H, Ar-CH_2-Ar), 4.14 (d, *J* = 18.6 Hz, 1H, Ar-CH_2-Ar), 4.1 (t, *J* = 7.2 Hz, 1H, CH), 7.1 – 7.3 (m, 8H, Ar-H). ^{13}C-NMR (75 MHz, $CDCl_3$): δ 32.30, 40.41, 45.32, 52.20, 56.21, 126.80, 128.71, 138.42, 140.10. Anal. ($C_{18}H_{21}N{\cdot}C_2H_2O_4{\cdot}0.5\ H_2O$): C, H, N.

4.1.10. *N*-methyl-2,2-diphenylethanamine (4b)—Yield (50%). mp 149 – 151 °C (oxalate) ^{1}H-NMR (300 MHz, $CDCl_3$): δ 2.47 (s, 3H, CH_3), 3.02 (d, *J* = 8.1 Hz, 2H, CH_2), 4.3 (t, *J* = 6 Hz, 1H, Ar-CH-Ar), 7.12 – 7.26 (m, 10H, Ar-H). ^{13}C-NMR (75 MHz, $CDCl_3$): δ 37.20, 44.80, 60.20, 126.60, 128.50, 129.60, 143.0. Anal. ($C_{15}H_{17}N{\cdot}C_2H_2O_4$): C, H, N.

4.1.11. *N*,*N*-dimethyl-3,3-diphenylpropan-1-amine (5c)—Yield (20%). mp 150 – 153 °C (oxalate) ^{1}H-NMR (300 MHz, $CDCl_3$): δ 2.52 – 2.56 (m, 2H, CH_2), 2.85 (s, 6H, $(CH_3)_2$), 3.0 – 3.02 (m, 2H, CH_2-N), 4.2 (t, *J* = 7.4 Hz, 1H, Ar-CH-Ar), 7.2 – 7.4 (m, 10H, Ar-H). ^{13}C-NMR (75 MHz, $CDCl_3$): δ 32.20, 45.80, 50.60, 58.33, 126.30, 128.20, 129.10, 143.15. Anal. ($C_{17}H_{21}N{\cdot}C_2H_2O_4{\cdot}0.5\ H_2O$): C, H, N.

4.1.12. 4,4-diphenylbutan-1-amine (6a)—Yield (60%). mp 198 – 200 °C (HCl) ^{1}H-NMR (300 MHz, $CDCl_3$): δ 1.42 – 1.48 (m, 2H, CH_2), 2.03 – 2.1 (m, 2H, CH_2), 2.73 (t, *J* =

NIH-PA Author Manuscript

NIH-PA Author Manuscript

NIH-PA Author Manuscript

6.2 Hz 2H, CH_2-NH_2), 4.1 (t, *J* = 7.2 Hz, 1H, Ar-CH-Ar), 7.1 – 7.3 (m, 10H, Ar-H). ^{13}C-NMR (75 MHz, $CDCl_3$): δ 32.30, 38.40, 42.30, 52.20, 126.80, 128.70, 129.40, 143.10. Anal. ($C_{16}H_{19}N$·0.5 HCl): C, H, N.

4.2. Molecular modeling

Molecular modeling investigations were conducted using the SYBYL 7.1 molecular modeling package (Tripos LP, St. Louis, MO) on MIPS R14K- and R16K-based IRIX 6.5 Silicon Graphics Fuel and Tezro workstations. Molecular mechanics-based energy minimizations were performed using the Tripos Force Field with Gasteiger-Hückel charges, a distance-dependent dielectric constant (ε = 4) and a non-bonded interaction cutoff of 8 Å and were terminated at an energy gradient of 0.05 kcal/(mol×Å). The hH_1 (P35367) and h5-HT_{2A} (P28233) receptor sequences were retrieved from the ExPASy Proteomics Server (http://www.expasy.org/) and aligned with a profile of several related class A GPCRs (human, dopamine D_3 (P35462), muscarinic cholinergic M_1 (P11229), vasopressin V_{1a} (P37288), adrenergic β_2 (P07550), δ-opioid (P41143), 5-HT_{2A} (P28223), dopamine D_2 (P14416), bovine rhodopsin (P02699) using the ClustalX program.[49] Within ClustalX, the slow-accurate alignment algorithm was used, the BLOSUM matrix series was employed and the gap opening penalty was increased from 10.0 to 15.0 to help maintain the continuity of the transmembrane helical segments. The alignment was carried out in two separate steps as reported by Bissantz, *et al.*[50] Manual adjustment of the ClustalX alignment was required to properly align the disulfide-forming cysteine residues in the EL2 loop. The result was an unambiguous alignment in the transmembrane (TM) helical regions of both the hH_1 and h5-HT_{2A} sequences with that of the β_2–adrenoceptor. This alignment, along with a file containing the atomic coordinates of the adrenergic β_2 receptor (PDB ID = 2RH1), was used as input to the MODELLER[40] software package to generate a population of 100 different hH_1 or h5-HT_{2A} homology models. Each of these receptors was subsequently energy-minimized.

The automated docking program GOLD[43] version 3.01 (Cambridge Crystallographic Data Centre, Cambridge, UK) was then used to dock the classical antihistaminic diphenhydramine and the high-affinity ligands **3c** and AMDA (**1a**) from the synthesized dihydroanthracene matrix into each of the 100 receptor models using the ChemScore fitness function. Based on the fitness function values, steric and electronic interactions of the docked poses and reported site-directed mutagenesis data, one receptor model was selected to represent the ligand binding site of the hH_1 and h5-HT_{2A} receptors. These models were subsequently analyzed using PROCHECK[51] and the ProTable facility within SYBYL to assess the geometric integrity of various structural elements (bond lengths, torsion angles, etc.) of each receptor model. After checks for stereochemical integrity, the receptor models were used for the docking of all the target compounds. Ligand molecules were created within SYBYL and energy-minimized using the same parameters as were used for the receptor models. Basic amines were protonated to form ammonium ions. GOLD was used to dock each resulting ligand structure (using the parameter set defined by the “standard default settings” option) into the final receptor model. Each receptor-ligand complex was then energy-minimized with its best-ranked docking pose.

The HINT scoring function was utilized (version 3.12) to explore and visualize hydropathic interactions by analyzing the ligand-receptor complexes generated by the automated docking program GOLD. The interaction scores were calculated for the highest-ranked ligand conformation. The receptors (5-HT_{2A} and H_1) and ligands were partitioned as distinct molecules. The ‘all hydrogen atoms’ option was employed in the H-bonding model, and hydrogen atoms at unsaturated positions and alpha to heteroatoms were considered potential H-bond donors. The inferred solvent model, which considers the partition of each residue based on its hydrogen count, was selected. The ‘Chain HBond Correction’ option was set to

NIH-PA Author Manuscript

NIH-PA Author Manuscript

NIH-PA Author Manuscript

'+20 –NH– SASA'. Finally, hydrophobic and polar interaction HINT maps were generated separately at +20% of the maximum HINT value.

4.3. Affinity determinations

Binding assays and data analysis were performed through the NIMH Psychoactive Drug Screening Program (PDSP) using cloned human receptors. The 5-HT_{2A} competitive binding assay employs [^{3}H]ketanserin (a 5-HT_{2A} antagonist) as the radioligand, and the H_1 competitive binding assay employs [^{3}H]chlorpheniramine (an H_1 antagonist) as the radioligand. Binding data were analyzed using Prism (GraphPad Software, Inc., San Diego, CA). Details of the binding assay protocol may be found at the PDSP home page, http://pdsp.med.unc.edu.

Acknowledgments

This work was supported by United States Public Health Service Grant R01-MH57969 (RBW), R01-GM71894 (GEK), NIMH Psychoactive Drug Screening Program (BLR) U19MH82441 (BLR) and RO1MH61887 (BLR).

References and notes

1. Ohayon MM. Sleep Med Rev. 2002; 6:97. [PubMed: 12531146]
2. Berger M, Gray JA, Roth BL. Annu Rev Med. 2009; 60:355. [PubMed: 19630576]
3. Popa D, Léna C, Fabre V, Prenat C, Gingrich J, Escourrou P, Hamon M, Adrien J. J Neurosci. 2005; 25:11231. [PubMed: 16339018]
4. Sanger DJ, Soubrane C, Scatton B. Ann Pharm Fr. 2007; 65:268. [PubMed: 17652996]
5. Barbier AJ, Bradbury MJ. CNS Neurol Disord Drug Targets. 2007; 6:31. [PubMed: 17305552]
6. Parmentier R, Ohtsu H, Djebbara-Hannas Z, Valatx JL, Watanabe T, Lin JS. J Neurosci. 2002; 22:7695. [PubMed: 12196593]
7. de Esch JP, Thurmond RL, Jongejan A, Leurs R. Trends Pharmacol Sci. 2005; 26:462. [PubMed: 16054239]
8. Smit MJ, Hoffmann M, Timmerman H, Leurs R. Clin Exp Allergy. 1999; 29(Suppl 3):19. [PubMed: 10444208]
9. Kakiuchi M, Ohashi T, Musoh K, Kawamura K, Morikawa K, Kato H. Jpn J Pharmacol. 1997; 73:291. [PubMed: 9165365]
10. Sangalli BC. Prog Neurobiol. 1997; 52:145. [PubMed: 9185237]
11. Welch, MJ.; Meltzer, EO.; Simons, FER. Histamine and H_1-Antihistamines in Allergic Disease. Simons, FER., editor. Marcel Dekker, Inc; New York: 2002.
12. Simons FER, Simons KJ. Clin Pharmacokinet. 1999; 36:329. [PubMed: 10384858]
13. Walsh GM, Annunziato L, Frossard N, Knol K, Levander S, Nicolas JM, Taglialatela M, Tharp MD, Tillement JP, Timmerman H. Drugs. 2001; 61:207. [PubMed: 11270939]
14. Nonaka H, Otaki S, Ohshima E, Kono M, Kase H, Ohta K, Fukui H, Ichimura M. Eur J Pharmacol. 1998; 345:111. [PubMed: 9593602]
15. Wieland K, Ter Laak AM, Smit MJ, Kühne R, Timmerman H, Leurs R. J Biol Chem. 1999; 274:29994. [PubMed: 10514483]
16. Westkaemper RB, Runyon SP, Bondarev ML, Savage JE, Roth BL, Glennon RA. Eur J Pharmacol. 1999; 380:R5. [PubMed: 10513561]
17. Runyon SP, Peddi S, Savage JE, Roth BL, Glennon RA, Westkaemper RB. J Med Chem. 2002; 45:1656. [PubMed: 11931619]
18. Westkaemper RB, Hyde EG, Choudhary MS, Khan N, Gelbar EI, Glennon RA, Roth BL. Eur J Med Chem. 1999; 34:441.
19. Runyon SP, Savage JE, Taroua M, Roth BL, Glennon RA, Westkaemper RB. Bioorg Med Chem Lett. 2001; 11:655. [PubMed: 11266163]

NIH-PA Author Manuscript

NIH-PA Author Manuscript

NIH-PA Author Manuscript

20. Cherezov V, Rosenbaum DM, Hanson MA, Rasmussen SGF, Thian FS, Kobilka TS, Choi HJ, Kuhn P, Weis WI, Kobilka BK, Stevens RC. Science. 2007; 318:1258. [PubMed: 17962520]
21. Westkaemper RB, Runyon SP, Savage JE, Roth BL, Glennon RA. Bioorg Med Chem Lett. 2001; 11:563. [PubMed: 11229772]
22. Lan P, Berta D, Porco JA Jr, South MS, Parlow JJ. J Org Chem. 2003; 68:9678. [PubMed: 14656094]
23. Lee H, Harvey RG. J Org Chem. 1990; 55:3787.
24. Bhattacharyya S. J Org Chem. 1995; 60:4928.
25. Klumpp DA, Sanchez GV Jr, Aguirre SL, Zhang Y, de Leon S. J Org Chem. 2002; 67:5028. [PubMed: 12098332]
26. Borch RF, Hassid AI. J Org Chem. 1972; 37:1673.
27. Jones G, Maisey RF, Somerville AR, Whittle BA. J Med Chem. 1971; 14:161. [PubMed: 5544405]
28. Clausen RP, Moltzen EK, Perregaard J, Lenz SM, Sanchez C, Falch E, Frølund B, Bolvig T, Sarup A, Larsson OM, Schousboe A, Krogsgaard-Larsen P. Bioorg Med Chem. 2005; 13:895. [PubMed: 15653355]
29. Casy, AF. Histamine and Anti-Histaminics. Rocha e Silva, M., editor. Vol. 18. Springer; Berlin: 1978. p. 215
30. Nauta, WT.; Rekker, RF. Histamine and Anti-Histaminics. Rocha e Silva, M., editor. Vol. 18. Springer; Berlin: 1978. p. 234
31. Zhang, M-Q.; Leurs, R.; Timmerman, H. Burger's Medicinal Chemistry and Drug Discovery. Wolff, ME., editor. Vol. 5. John Wiley & Sons; New York: 1997. p. 495
32. Harms, AF.; Hespe, W.; Nauta, WT.; Rekker, RF.; Timmerman, H.; de Vries, J. Drug Design. Ariëns, EJ., editor. Vol. 6. Academic Press; New York: 1975. p. 1
33. Timmerman, H. Analogue-Based Drug Discovery. Fischer, J.; Ganellin, CR., editors. Wiley-VCH; Weinheim: 2006. p. 401
34. Duarte CD, Barreiro EJ, Fraga CAM. Mini-Rev Med Chem. 2007; 7:1108. [PubMed: 18045214]
35. Allaby RG, Woodwark M. Evol Bioinform. 2007; 3:155.
36. Choudhary MS, Craigo S, Roth BL. Mol Pharmacol. 1993; 43:755. [PubMed: 8388989]
37. Choudhary MS, Sachs N, Uluer A, Glennon RA, Westkaemper RB, Roth BL. Mol Pharmacol. 1995; 47:450. [PubMed: 7700242]
38. Roth BL, Choudhary MS, Khan N, Uluer AZ. J Pharmacol Exp Ther. 1997; 280:576. [PubMed: 9023266]
39. Roth BL, Shoham M, Choudhary MS, Khan N. Mol Pharmacol. 1997; 52:259. [PubMed: 9271348]
40. Fiser, A.; Šali, A. Methods in Enzymology: Macromolecular Crystallography: Part D. Carter, CWJ.; Sweet, RM., editors. Vol. 374. 2003. p. 461
41. The Ballesteros-Weinstein residue index (see Ballesteros JA, Weinstein H. Methods Neurosci. 1995; 25:366.and Xhaard S, et al. J Struct Biol. 2005; 150:126. [PubMed: 15866736]) is used throughout this work to identify residues at specific positions within the transmembrane helical (TM) regions. Individual amino acids are specified by their one-letter residue abbreviation and primary sequence position followed by the Ballesteros-Weinstein index as a superscript.
42. Javitch JA, Ballesteros JA, Weinstein H, Chen J. Biochemistry. 1998; 37:998. [PubMed: 9454590]
43. Jones G, Willett P, Glen RC, Leach AR, Taylor R. J Mol Biol. 1997; 267:727. [PubMed: 9126849]
44. Kellogg GE, Semus SF, Abraham DJ. J Comput-Aided Mol Des. 1991; 5:545. [PubMed: 1818090]
45. Cozzini P, Fornabaio M, Marabotti A, Abraham DJ, Kellogg GE, Mozzarelli A. J Med Chem. 2002; 45:2469. [PubMed: 12036355]
46. Runyon SP, Mosier PD, Roth BL, Glennon RA, Westkaemper RB. J Med Chem. 2008; 51:6808. [PubMed: 18847250]
47. Jongejan A, Leurs R. Arch Pharm Chem Life Sci. 2005; 338:248.
48. Almaula N, Ebersole BJ, Zhang D, Weinstein H, Sealfon SC. J Biol Chem. 1996; 271:14672. [PubMed: 8663249]
49. Chenna R, Sugawara H, Koike T, Lopez R, Gibson TJ, Higgins DG, Thompson JD. Nucleic Acids Res. 2003; 31:3497. [PubMed: 12824352]

NIH-PA Author Manuscript

NIH-PA Author Manuscript

NIH-PA Author Manuscript

50. Bissantz C, Bernard P, Hilbert M, Rognan D. Proteins. 2003; 50:5. [PubMed: 12471595]
51. Laskowski RA, MacArthur MW, Moss DS, Thornton JM. J Appl Crystallog. 1993; 26:283.
52. Ballesteros JA, Weinstein H. Methods Neurosci. 1995; 25:366.
53. Barton GJ. Protein Eng. 1993; 6:37. [PubMed: 8433969]

NIH-PA Author Manuscript

NIH-PA Author Manuscript

NIH-PA Author Manuscript

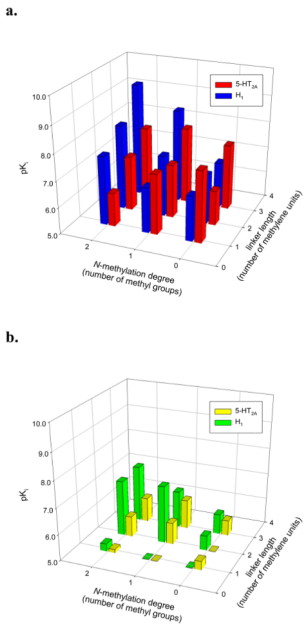

Figure 1.

3D bar graph showing the affinities at 5-HT_{2A} and H_1 for the **a**) 9-(aminoalkyl)-9,10-dihydroanthracene (DHA) and **b**) diphenylalkylamine (DPA) analogs listed in Table 1.

NIH-PA Author Manuscript
NIH-PA Author Manuscript
NIH-PA Author Manuscript

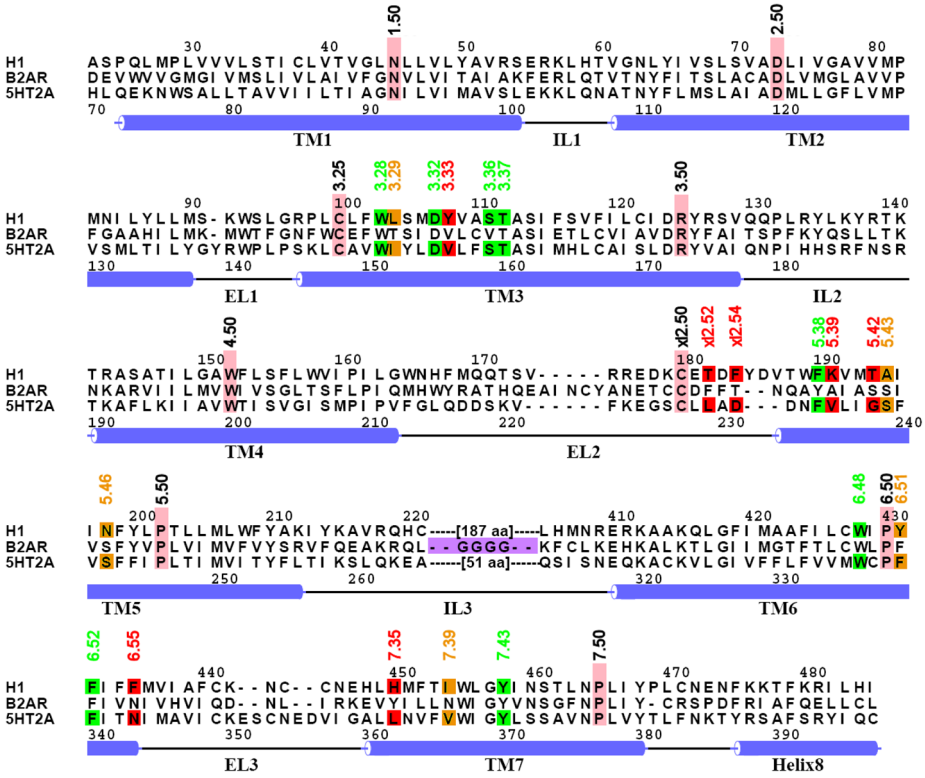

Figure 2.

Alignment of the human β_2-adrenergic, H_1 and 5-HT_{2A} receptor sequences. Sequence positions highlighted in pink indicate highly conserved amino acids among the Class A GPCR family that serve as reference positions in the Ballesteros-Weinstein[52] numbering system, as well as the cysteine residues of the disulfide bridge tethering EL2 to TM3. The traditional numbering shown corresponds to the hH_1 (top) and h5-HT_{2A} (bottom) sequences. β_2-Adrenergic residues highlighted in purple indicate positions in the third intracellular loop (IL3) that were mutated to glycine in the hH_1 and h5-HT_{2A} sequences; these were retained in subsequent hH_1 and h5-HT_{2A} models. Other residues highlighted in the hH_1 and h5-HT_{2A} sequences represent the residues of the binding site and correspond to those positions that are within 5.0 Å of the carazolol ligand bound in the β_2AR homolog. The color indicates the degree of similarity between the hH_1 and h5-HT_{2A} residue at a particular position as defined by the Gonnet PAM250 similarity matrix (green = identical; yellow = strong or weak conservation; red = no conservation). The figure was created using ALSCRIPT.[53]

NIH-PA Author Manuscript

NIH-PA Author Manuscript

NIH-PA Author Manuscript

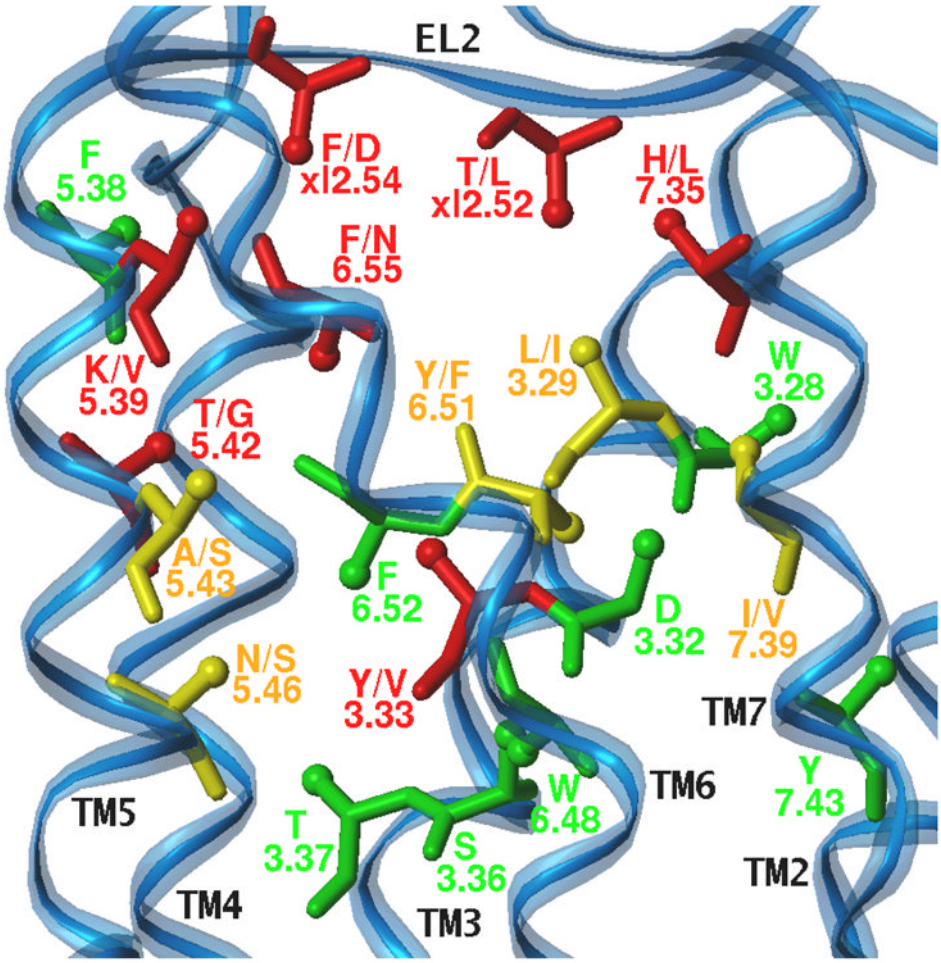

Figure 3.

Illustration of the differences in binding site residue composition of the hH_1 and h5-HT_{2A} receptors within the context of the β_2AR-T4L crystal structure. Residues are truncated at the C^{β} carbon atom (ball-and-stick representation) and are colored based on residue similarity as described in Fig. 2. For those positions whose residue identity differs, the H_1 residue is listed first, followed by the 5-HT_{2A} residue.

NIH-PA Author Manuscript

NIH-PA Author Manuscript

NIH-PA Author Manuscript

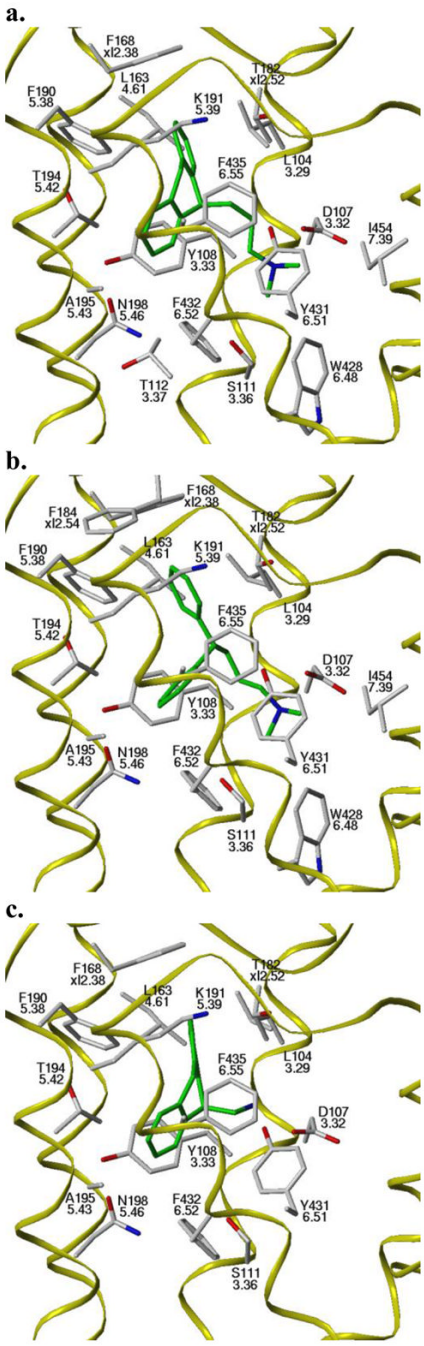

Figure 4.

Docked hH_1-ligand complexes. **a**) **3c. b**) **6c. c**) **1a**. Residues within 5 Å of the bound ligand are displayed.

NIH-PA Author Manuscript

NIH-PA Author Manuscript

NIH-PA Author Manuscript

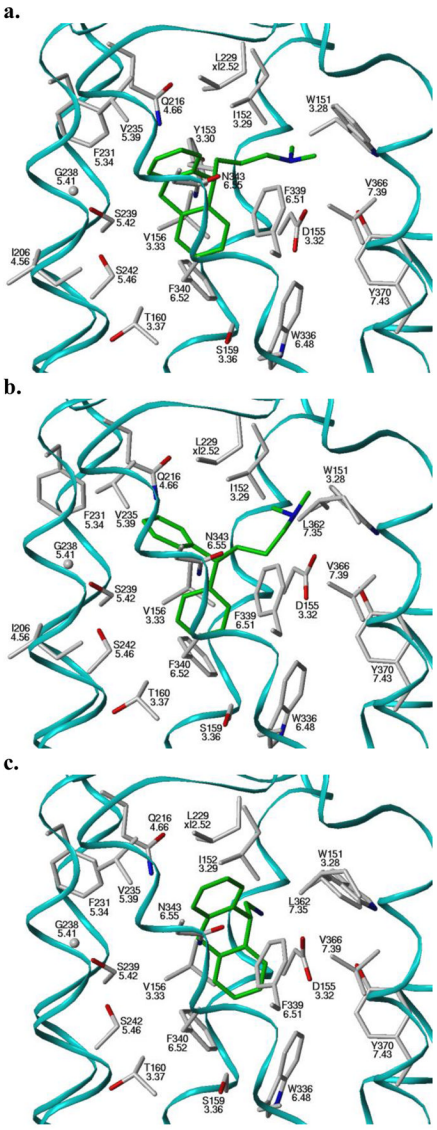

Figure 5.

Docked h5-HT_{2A}-ligand complexes. **b**) **3c. b**) **6c**. c) **1a**. Residues within 5 Å of the bound ligand are displayed.

NIH-PA Author Manuscript

NIH-PA Author Manuscript

NIH-PA Author Manuscript

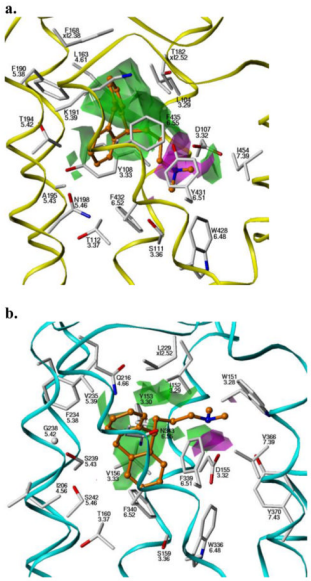

Figure 6.
HINT interaction maps for compound **3c** in a) H_1 and b) 5-HT_{2A} binding sites. Regions of favorable hydrophobic (green) and polar (magenta) intermolecular interactions are shown as contours.

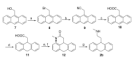

Scheme 1.

(a) PBr_3, toluene 0 °C, 1 h; (b) KCN, DMSO, 70 °C, 1 h; (c) KOH, ethylene glycol:H_2O (1:1), reflux, 12 h; (d) Na, 1-pentanol, reflux, 30 min; (e) $SOCl_2$, dry benzene, reflux, 2 h; (f) methylamine-THF, 25 °C, 6 h; (g) BH_3·THF, THF reflux, 6 h.

NIH-PA Author Manuscript
NIH-PA Author Manuscript
NIH-PA Author Manuscript

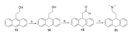

Scheme 2.

(a) Na_2K silica gel, THF, 1 h; (b) Dess-Martin reagent, CH_2Cl_2, 1 h; (c) Me_2NH HCl, Ti(O-*i*-Pr)$_4$, NEt_3, Abs. EtOH, 25 °C, 9 h, $NaBH_4$, 25 °C, 10 h.

NIH-PA Author Manuscript

NIH-PA Author Manuscript

NIH-PA Author Manuscript

NIH-PA Author Manuscript
NIH-PA Author Manuscript
NIH-PA Author Manuscript

Bioorg Med Chem. Author manuscript; available in PMC 2011 May 5.

Table 1

Observed binding affinities for 9-(aminoalkyl)-9,10-dihydroanthracene (DHA) and diphenylalkylamine (DPA) analogs at 5-HT_{2A} and H_1 receptors.

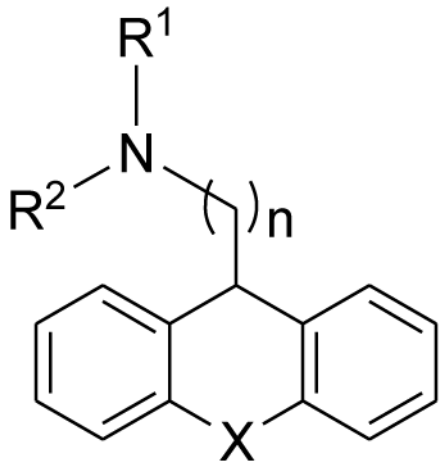

					K_i (nM)	
Cpd.	**X**	**n**	**R^1**	**R^2**	**5-HT_{2A}**	**H_1**
1a	–CH_2–	1	–H	–H	20[a]	197
b	–CH_2–	1	–H	–CH_3	52[b]	189
c	–CH_2–	1	–CH_3	–CH_3	540[b]	25
2a	–CH_2–	2	–H	–H	480[b]	137
b	–CH_2–	2	–H	–CH_3	92	48
c	–CH_2–	2	–CH_3	–CH_3	84	6
3a	–CH_2–	3	–H	–H	32[b]	175
b	–CH_2–	3	–H	–CH_3	13	3
c	–CH_2–	3	–CH_3	–CH_3	22	0.5
4a	–H, –H	1	–H	–H	4610[c]	>10,000
b	–H, –H	1	–H	–CH_3	>10,000	>10,000
c	–H, –H	1	–CH_3	–CH_3	7356	5172

Cpd.	X	n	R^1	R^2	K_i (nM)	
					5-HT_{2A}	H_1
5a	–H, –H	2	–H	–H	>10,000	2758
b	–H, –H	2	–H	$–CH_3$	1498	64
c	–H, –H	2	$–CH_3$	$–CH_3$	1636	75
6a	–H, –H	3	–H	–H	2589	1670
b	–H, –H	3	–H	$–CH_3$	754	386
c	–H, –H	3	$–CH_3$	$–CH_3$	1151	70

[a] From Westkaemper, et al. 2001.[21]

[b] From Runyon, et al. 2001.[19]

[c] From Runyon, et al. 2002.[17]

NIH-PA Author Manuscript NIH-PA Author Manuscript NIH-PA Author Manuscript